Effects of Magnetic Topology on Axisymmetric Divertors

Halima Ali[1], Alkesh Punjabi[1], and Allen Boozer[2]

[1]*Hampton University, Hampton, VA 23668, USA*

[2]*Columbia University, New York, NY 10227, USA*

ABSTRACT: The effects of the magnetic topology on the axisymmetric divertor are investigated. Two distinct magnetic topologies are studied: the open-unbounded and the closed-compact. Open-unbounded magnetic topology is represented by the simple map and the closed-compact topology by the symmetric quartic map. Identical magnetic perturbation is applied and field lines are given a constant artificial radial spiraling velocity. Preliminary results of the study are presented. How the confinement time and the loss time of the field lines for unperturbed and perturbed axisymmetric divertors are calculated and compared for both topologies.

Single-null divertor tokamaks can have two distinct topologies – the open and unbounded topology or the closed and compact topology. For both of these topologies, the unperturbed magnetic surfaces inside the separatrix are closed. For the open and unbounded topology, the magnetic surfaces outside the separatrix are open. For the closed and compact topology, the separatrix is in the shape of figure eight, and the magnetic surfaces outside the separatrix are also closed, Figs 1(a-b). The simple map (SM) [1] is the simplest symplectic map that generically represents the open-unbounded topology; and the symmetric quartic map (SQM) [2] is the simplest symplectic map that generically represents the closed-compact topology. SQM's generating function contains three positive parameters in its coefficients which control the height and width of ideal separatrix surface and poloidal magnetic flux inside ideal separatrix. In this paper, these maps are used to study the effects of topology on the axisymmetric divertor. Natural canonical coordinates [3] are used for both maps. The parameters in the SQM are chosen so that: (1) the unperturbed poloidal fluxes inside the separatrix is the same for both topologies, $\bar{\psi}_p(\psi_t,\theta)=1/6.$; (2) the widths and the heights of the separatrix surfaces are approximately the same for both topologies, Fig. 1(c). The generating function in NCC for the SM is given by $\bar{\psi}_p(\psi_t,\theta)=\psi_t+(2\sqrt{2}/3)\psi_t^{3/2}\sin^3(\theta)$, and for the SQM by $\bar{\psi}_p(\psi_t,\theta)=a(\theta)\psi_t^2+b(\theta)\psi_t^{3/2}+c(\theta)\psi_t+d$, where $a(\theta)=(128/243)\sin^4(\theta)$, $b(\theta)=(32/27)\sin^2(\theta)$, $c(\theta)=(32/27)\sin^2(\theta)+(27/64)\cos^2(\theta)$, and $d=-1/6$. ψ_t is toroidal flux and θ is poloidal angle. The equilibrium axisymmetric magnetic geometries from these generating functions are

shown in Figs. 1(a,b). Total poloidal flux is $\psi_p(\psi_t,\theta,\varphi)=\bar{\psi}_p(\psi_t,\theta)+\tilde{\psi}_p(\psi_t,\theta,\varphi)$ where $\tilde{\psi}_p$ is the magnetic perturbation, and φ is the toroidal angle. Magnetic perturbation is given by $\tilde{\psi}_p(\psi_t,\theta,\varphi)=\Sigma_{(m,n)}\delta_{mn}(\psi_t)\cos(m\theta-n\varphi)$ where m and n are poloidal and toroidal mode numbers of the Fourier modes. Poloidal flux ψ_p is the Hamiltonian function for the trajectories of magnetic field lines. The symplectic map equations are calculated from the canonical transformation $\psi_t^{(j+1)}=\psi_t^{(j)}-k\partial\psi_p(\psi_t^{(j+1)},\theta^{(j)},\varphi^{(j)})/\partial\theta^{(j)}$, $\theta^{(j+1)}=\theta^{(j)}+k\partial\psi_p(\psi_t^{(j+1)},\theta^{(j)},\varphi^{(j)})/\partial\psi_t^{(j+1)}$, and $\varphi^{(j+1)}=\varphi^{(j)}+k$. j is the iteration number. k is the step-size of the symplectic integration; here $k=2\pi/360$ for both maps. The perturbation is chosen to have mode numbers $(m,n)=(3,1)+(4,1)$ with amplitude $\delta=5\times10^{-3}$ in both maps. The radial dependence of the perturbation is ignored. The outermost confining surface for the SM is through $x=0$, $y_{LGS}=0.833$; and for the SQM is $x=0$ and $y_{LGS}=0.756$. The widths of the stochastic layers near the X-points are $w/r_{SEP}\approx0.17$ for the SM and $w/r_{SEP}\approx0.29$ for the SQM. The width of the SQM is about 1.7 times that of the SM for the same perturbation. The phase portraits of the SM and SQM with these perturbations in the poloidal plane $\varphi=0$ are shown in Fig. 2.

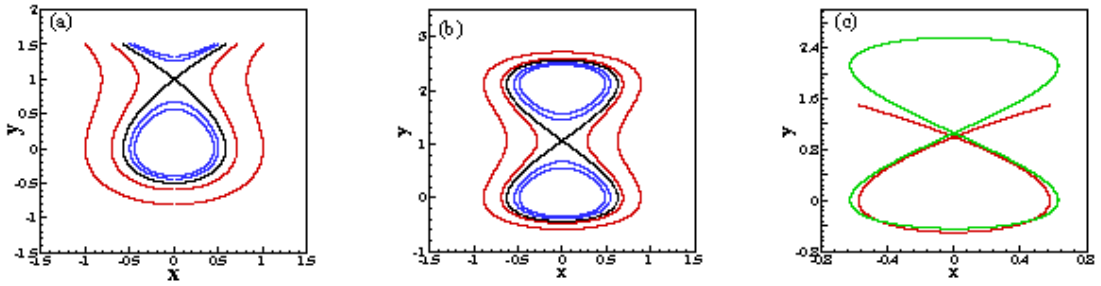

Fig. 1: Topologies of axisymmetric divertor in the SM and the SQM. (a) Open and unbounded topology represented by SM, (b) Closed and bounded topology represented by SQM, (c) Comparison of the separatrices of the SM and SQM.

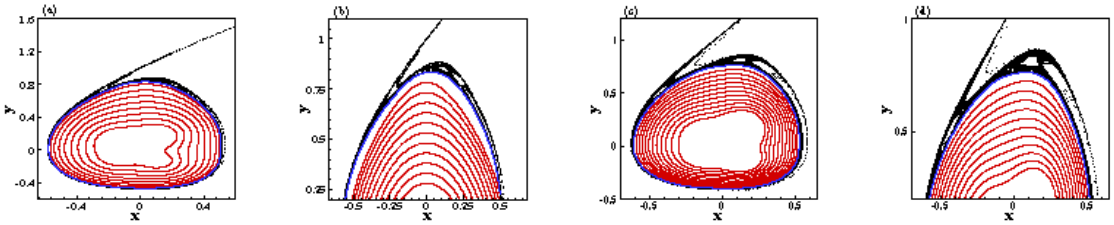

Fig. 2: Phase Portraits of SM (a,b) and SQM (c,d) and their close-up views when $\delta=5\times10^{-3}$. In both cases, these figures depict the outermost confining surfaces, islands, closed confining surfaces and magnetic turnstiles.

A field line is started on the outermost confining surface in the plane $\varphi=0$ in the SM and advanced for 10,000 toroidal circuits and every tenth point in the $\varphi=0$ plane is chosen as an initial condition. The same procedure is used to choose initial conditions on the outermost confining surface in the SQM. In each case, the 1,000 lines are advanced for 10,000 toroidal circuits. The filed lines are given a radial velocity of D per radian of toroidal advance in the

ψ_t-space. After each iteration of the field line, ψ_t is changed to ψ_t+kD. D is varied from 1×10^{-6}, 9×10^{-5}, 8×10^{-5}, …,1×10^{-2}. This causes the field lines to spiral out radially. Radial spiraling of field lines is used to simulate the escape of field lines through magnetic turnstiles. The stochastic region outside the outermost confining surface is made up of islands, chaos, and cantori. The field lines escape by threading through the gaps or holes in cantori also called magnetic turnstiles. In the vicinity of one cantorus, there is an infinite Markov tree of cantori, which slow the escape of magnetic field lines and cause the lines to linger or stick in that region for many toroidal circuits. An infinite Markov tree of cantori means that there are an infinite number of cantori with which the trajectory interacts and that the trajectory can be assumed to interact with the various cantori in a random (Markovian) manner [4-5]. This is an extremely complicated process. The walls are placed in planes though the X-points and are orthogonal to the lines joining the O-points to the X-points in both topologies. The strike points are calculated from the respective continuous analogs of the maps if the line strikes the wall during an iteration of the map; otherwise if the line strikes the wall during the radial spiraling, it is easy to calculate the strike points analytically. In this way, the footprints on walls are calculated for different values of the spiraling velocity D. Depending on the values of the spiraling velocity, the footprints for the closed and bounded topology (SQM) form different structures with sharp boundaries and interior structures. Fig. 3 shows the three typical structures that occur. These are shown in Fig. 3 for the values $D=3\times10^{-4}$, $D=2\times10^{-3}$, and $D=1\times10^{-2}$. For the open and unbounded topology (SM) similar structures develop with different ranges of the spiraling velocity and the scalings in the x-direction. In future, we plan to do a detailed study of the sizes, shapes, and structures of footprints for both topologies.

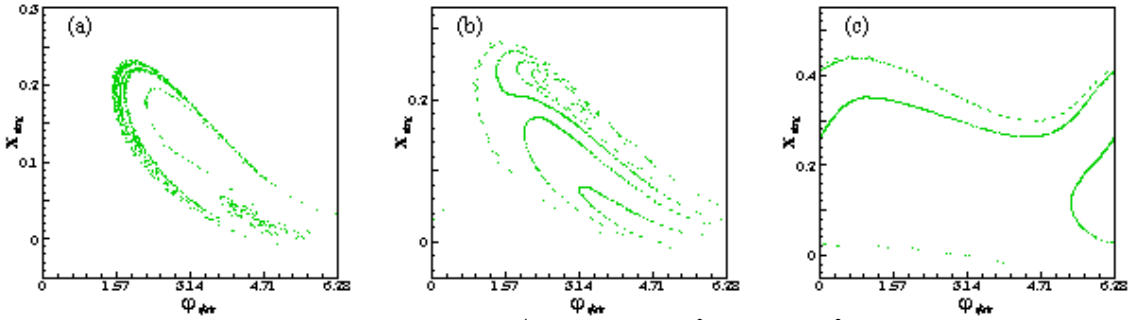

Fig. 3: The footprint for the SQM when (a) $D=3\times10^{-4}$ and (b) $\delta=2\times10^{-3}$. (c) $\delta=1\times10^{-2}$.

During the 10,000 toroidal circuits' journey of the field lines with radial spiraling through the magnetic turnstiles, the first line strikes the wall after a toroidal advance of φ_0 radians. φ_0 is full confinement time because all lines are confined during this time. For both topologies, Fig. 4 shows the scalings of φ_0 with respect to D when the perturbation amplitude

δ=0 and δ =5×10^{-3}. For unperturbed axisymmetric divertor, φ_0 scales as 1/D, and for highly perturbed axisymmetric divertor, φ_0 scales as D to the power -½. This is true for both topologies.

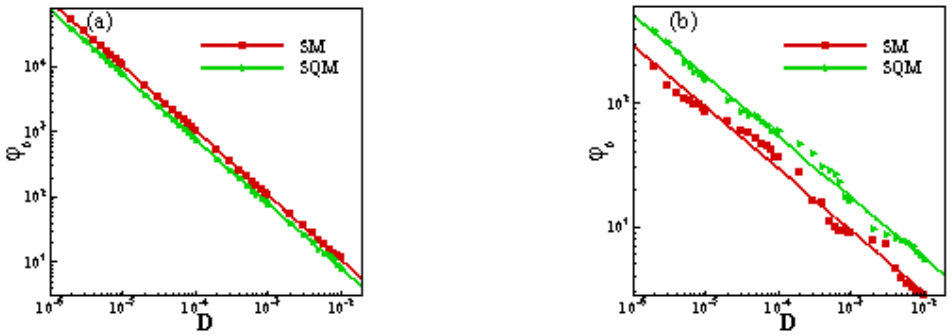

Figs. 4: Scaling of φ_0 as a function of radial velocity D for SM and SQM: (a) when δ=0, and (b) when δ=5×10^{-3}. In both cases φ_0 scales as 1/D when δ=0 and the square root of radial velocity $\sqrt{D}$ when δ=5×10^{-3}.

The loss time φ_{LOSS} is defined as the time it takes the number of confined lines to drop to 1/e of the starting number of lines. For unperturbed axisymmetric divertor, φ_{LOSS} scales as D to the power -1/10 for the open topology (SM) and -1/8 for the closed topology (SQM). For axisymmetric divertor with high perturbation, δ=5×10^{-3}, the loss time φ_{LOSS} scales as $D^{-2/5}$ for open topology (SM) and as $D^{-1/2}$ for closed topology (SQM), Fig. 5.

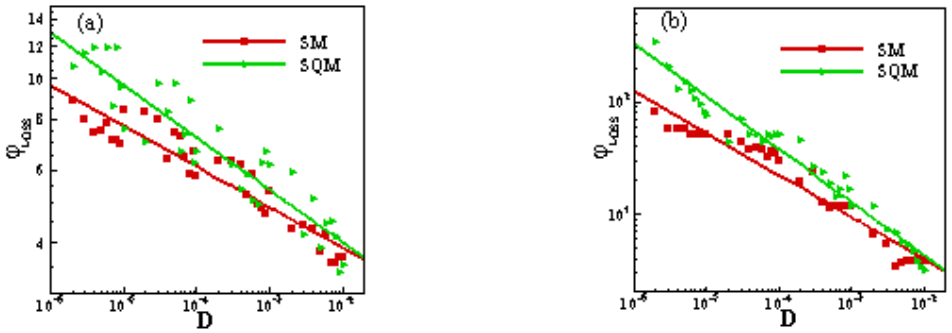

Fig. 5: The loss time φ_{LOSS} as a function of D for SM and SQM (a) when δ=0, and (b) when δ=5×10^{-3}. When δ=0, φ_{LOSS} scales as D to the power -1/10 the SM and -1/8 for the SQM. For high perturbation, δ=5×10^{-3}, the loss time φ_{LOSS} scales as $D^{-2/5}$ for the SM and as $D^{-1/2}$ for the SQM

Acknowledgments: This work is supported by the US DOE grants DE-FG02-01ER54624 and DE-FG02-04ER54793. NERSC resources under contract DE-AC02-05CH11231 is used to carry-out calculations.

References

[1] A. Punjabi, A. Verma, and A. Boozer, *Phys. Rev. Lett*. **69**, 3322 (1992).

[2] M. Jones et al, *Phys. Plasmas* **16**, 042511 (2009).

[3] A. Punjabi, *Nucl. Fusion* **49**, 115020 (2009).

[4] A. H. Boozer and A. Punjabi, *Phys. Plasmas* **23**, 102513 (2016).

[5] Simulation of stellarator divertors, A. H. Boozer and A. Punjabi, submitted for publication.